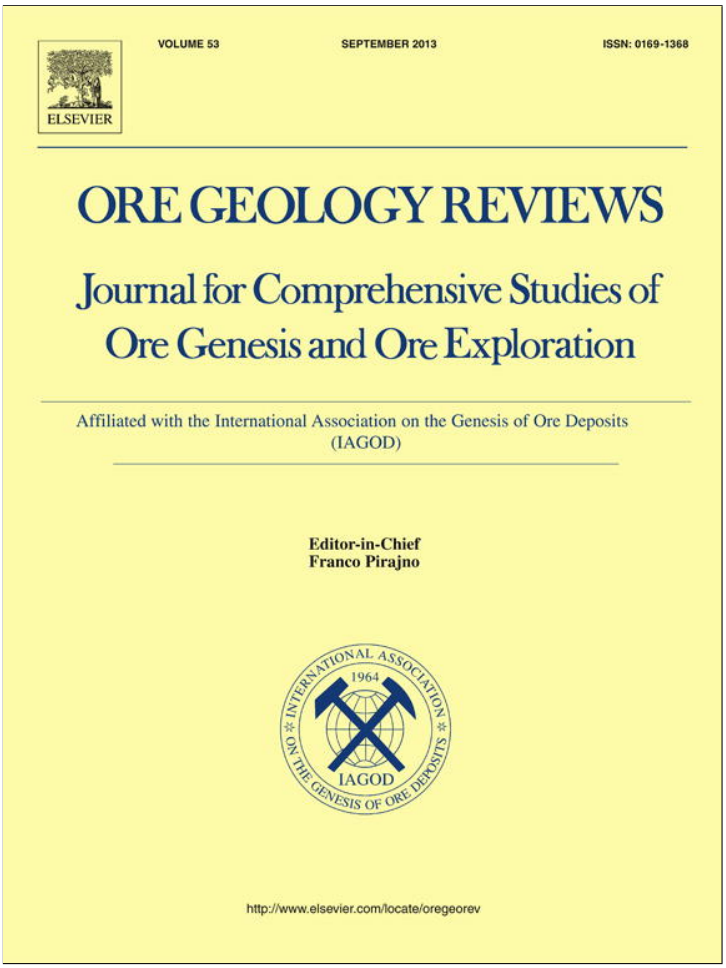

Ore Geology Reviews 53 (2013) 276–286

Contents lists available at SciVerse ScienceDirect

Ore Geology Reviews

journal homepage: www.elsevier.com/locate/oregeorev

Noble metal-graphite mineralization: A comparative study of the carbonaceous granite-gneiss complex and shales of the Russian Far East

Alexander I. Khanchuk [a], Victor P. Nechaev [a,*], Laura P. Plyusnina [a], Nikolay V. Berdnikov [b], Vladimir P. Molchanov [a], Sergei V. Vysotskiy [a]

[a] Far East Geological Institute, Far Eastern Branch, Russian Academy of Sciences, 159, Pr. Stoletiya Vladivostoka, Vladivostok, 660022, Russia
[b] Kosygin Institute of Tectonics and Geophysics, Far Eastern Branch, Russian Academy of Sciences, 65, Ul. Kim Yu Chena, Khabarovsk, 680000, Russia

ARTICLE INFO

Article history:
Received 1 June 2011
Received in revised form 28 November 2011
Accepted 29 January 2013
Available online 5 February 2013

Keywords:
Platinum
Gold
Graphite
Mantle
Fluid

ABSTRACT

A new noble metal-graphite mineralization has been revealed in the Ruzhino amphibolite-facies rocks of the northern Khanka block. It is characterized by Au and PGE (platinum group elements) contents (up to tens g/t, Pt > Au) as high as those in world-class deposits hosted by sedimentary and magmatic rocks, but is distinguished from them by isotopic composition of carbon, hydrogen and oxygen, all suggesting a distinct mantle contribution ($\delta^{13}C_{VPDB}$ from −8.5 to −10.5‰ in graphite, δD_{VSMOW} from −82.5 to −106.7‰ and $\delta^{18}O_{VSMOW}$ from 8.2 to 10.1‰ in biotite). The Ruzhino-type mineralization is highly resistant to common chemical treatments, so that detection of their metals requires that some special methods be developed. Atomic Absorption Spectrophotometry and Inductively Coupled Plasma Mass Spectrometry following severe chemical treatments and ignition at 600–650 °C, as well as Ion Mass Spectrometry allowing a direct detection of elements in solid materials were employed in this study. These methods increased noble-metal contents of the graphitized rocks compared to standard analyses including a conventional fire assay. In addition, electron microscopy surveys discovered extremely diverse native-metal and intermetallic complexes with C, O, Cl, F, REE and other elements. The microinclusions, however, represent a minor part of the mineralization. Major constituents seem to form carbonaceous nanocompounds invisible under a microscope. These graphite-based nanocomplexes, which are especially developed in the case of Pt, seem to be responsible for the highly resistant character of the Ruzhino mineralization. They also may be present in the latent form among the common Au ± PGE ores hosted by carbonaceous shales like those we studied in the close vicinity of the Ruzhino amphibolite-facies rocks and in the northeastern Bureya–Jiamusi terrane.

1. Introduction

Noble-metal mineralization is well known in carbon-bearing sedimentary and magmatic rocks commonly metamorphosed at the greenschist facies. This is true for many of world-class deposits, including Bushveld, South Africa (Ballhaus and Stumpfl, 1985), Stillwater, U.S.A. (Volborth and Housley, 1984), Sudbury, Ontario, Canada (Wright et al., 2010), Kempirsai, Kazakhstan (Melcher et al., 1997), Sukhoi Log, Russia (Distler et al., 2004; Razvozzhaeva et al., 2008), Macraes, New Zealand (Craw, 2002), Carlin-type deposits in USA and China (Li and Peters, 1998), Coronation Hill and other epithermal sediment-hosted deposits in Australia and Brazil (Mernagh et al., 1994; Sener et al., 2002), and many others. What is more, carbon is considered to play a significant role in ore-forming processes, in particular the transportation of noble metals by C − O − H ± S ± Cl ± F fluids and their precipitation under the reducing influence of organic matter and graphite in host rocks (Ballhaus and Stumpfl, 1985; Boudreau and McCallum, 1992; Hulen and Collister, 1999; Mogessie et al., 1991; Pasava, 1993). This is supported by many experimental studies that have shown an ability of carbon to form compounds with gold and PGE under hydrothermal and sedimentary conditions (Bittencourt et al., 2008; Dunaev et al., 2008; Kubrakova et al., 2010; Plyusnina et al., 2000, 2004, 2009; Tressaud and Hagenmuller, 2001; Varshal et al., 2000). However, the major economic value of noble-metal ores is currently based on carbon-free minerals such as native precious metals, their alloys with base metals, sulfides, and oxides, as well as arsenides, tellurides, bismuthides, selenides, and antimonides (Daltry and Wilson, 1997; Kaukonen, 2008; Naldrett et al., 2008). Their particles are commonly hosted by or intergrown with quartz and other silicates, as well as base-metal sulfides and oxides. Compounds of noble metals with carbon and/or noble-metal minerals in a direct contact with hydrocarbons, amorphous carbon, or graphite are, on the other hand, quite rarely reported (e.g., Berdnikov et al., 2010; Crespo et al., 2006; Khanchuk et al., 2007; Kucha, 1981; Kucha and Plimer, 1999; Kucha and Przybylowicz, 1999).

How to explain this? Two possible scenarios exist: either the natural affinity between carbon and noble metals is not implemented in

* Corresponding author. Tel.: +7 4232 318750; fax: +7 4232 317847.
E-mail address: vnechaev@hotmail.com (V.P. Nechaev).

0169-1368/$ – see front matter © 2013 Elsevier B.V. All rights reserved.
http://dx.doi.org/10.1016/j.oregeorev.2013.01.013

ores for some unknown reason, or the methods commonly applied to detect and extract carbon-bound metals are imperfect. Our studies of graphite-associated noble-metal mineralization, the results of which have been published primarily in Russian and partly translated into English (Khanchuk et al., 2004, 2007, 2009, 2010a,b), will be reviewed and summarized in this paper along with a presentation of our most recent data in order to illuminate the scientific and, possibly, economic issues of this problem. In addition, the paper develops interpretations based on all data collected.

2. Geological setting

Graphite-bearing rocks of various metamorphic grades, all located in the Bureya–Jiamusi–Khanka superterrane at the eastern termination of the Central-Asian Orogenic Belt, were the subject of the present research (Fig. 1). This superterrane is composed of the late Pan-African (500–525 Ma) granite-metamorphic complexes overlapped by the Middle Paleozoic–Jurassic subduction-related volcano-sedimentary units, collisional and post-collisional dynamo-metamorphic formations and related magmatic complexes (Dacheng et al., 2004; Khanchuk et al., 2010a,b; Mishkin et al., 2000; Wilde and Wu, 2003; Wu et al., 2007; Zhou et al., 2010). The protolith of the Pan-African metamorphic rocks has Rb – Sr, Sm – Nd and U – Pb ages ranging from 700 to 1000 Ma with a single zircon date as old as 2090 Ma, suggesting that the Khanka and Bureya–Jiamusi blocks were jointly derived from either Gondwana or the North Asian Craton (Wilde and Wu, 2003; Zhou et al., 2010). The blocks collided with the Sino-Korean Craton in the Late Permian-Early Triassic (Dacheng et al., 2004) and with the Songliao block of Central-Asian Orogenic Belt, during the Triassic-Early Jurassic (Zhou et al., 2010). Some magmatic events occurred in the region in the Mid Paleozoic time (Tsygankov et al., 2010) including intrusions of granitic and alkaline rocks associated with rare-metal-fluorite mineralization in the Voznesenka Terrane (Krymsky and Belyatsky, 2001; Sato et al., 2003).

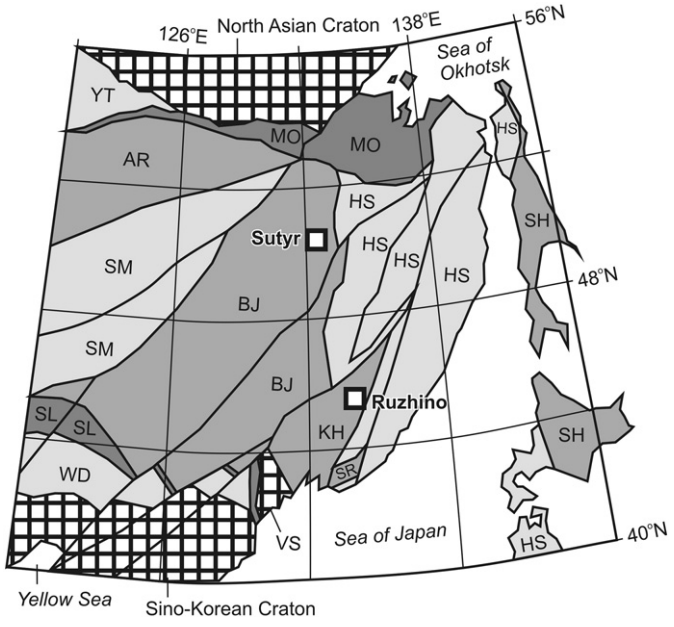

Fig. 1. The East Asia terrane scheme (simplified after Khanchuk, 2001) showing the Ruzhino and Sutyr locations (see Figs. 2 and 3 for details). Terrane abbreviations: VS — Voznesenka (Archean–Permian); BJ and KH — Bureya–Jiamusi and Khanka (Late Proterozoic–Permian), SR — Sergeevka (Cambrian–Ordovician); YT — Yenisey–Transbaikal (Vendian to Early Ordovician), MO — Mongol–Okhotsk (Devonian to Late Jurassic), AR — Argun–Idermeg (Late Proterozoic–Cambrian), SM — South Mongolia–Khingan (Ordovician to Carboniferous), SL — Solon (Carboniferous to Permian), WD — Wundurmiao (Riphean to Ordovician), HS — Honshu–Sikhote–Alin (Jurassic to Early Cretaceous), SH — Sakhalin–Hokkaido (Cretaceous).

2.1. Khanka terrane

Graphite-bearing metamorphic rocks of the northern Khanka terrane serve as a central subject of our study. They were sampled at quarries in the Lesozavodsk graphitization district, 1900 km^2 in size, established as a result of exploration performed in the middle of the 20th Century (Solonenko, 1951). We have named this area the Ruzhino noble-metal occurrence, including the Turgenevo and Tamga graphite deposits. The graphite mineralization is hosted by Proterozoic–Cambrian volcano-sedimentary rocks metamorphosed into granulites, amphibolites and green schists there.

The granulites and amphibolites form cores of narrow, tightly compressed folds of latitudinal and less often northwestern and northeastern orientation, enclosed in the larger dome-like structures, all cut by numerous faults of different strike. Gabbro and granite intrusions of the Mid Paleozoic–Mesozoic age outline the dome structure and occupy its center, whereas the Lower Paleozoic granite seems to be distributed independently.

The Ruzhino noble-metal occurrence particularly is dominated by amphibolite-facies rocks including intercalation of garnet-biotite-feldspar and biotite-quartz-feldspar crystalline schists with marble. There also are conformable injections of biotite and leucocratic granites, some of which are rich in K, as well as thin (up to 1 m) dikes of K-rich syenitic lamprophyre. Marble is altered into garnet-diopside skarn at the contacts with granite. Carbonaceous green schist-facies rocks, outcropped at the southern edge of the Ruzhino occurrence, were involved in our study for comparison. They are composed of fine-crystalline quartz, sericite, amorphous carbon, and graphite (total carbon up to 12%) with some admixture of chlorite. We will conventionally call them carbonaceous shale, black shale or just shale to emphasize their principal difference from the amphibolite-facies schists noted above.

2.2. Bureya–Jiamusi terrane

Carbonaceous shales were sampled on the left bank of the Sutyr River, the northeastern Bureya–Jiamusi terrane (Fig. 1). These rocks belong to the Upper Riphean–Lower Cambrian formation consisting of mudstones, phthanites, siltstones, sandstones, limestones, dolomites, jasper-like rocks, magnetite-hematite ores, rhyolites, rhyolitic tuffs, and basalts of 1800–2000 m in total thickness. The shales contain disseminated organic matter (1–22%) with some addition of graphite flakes 0.001–0.03 mm in size (Berdnikov et al., 2010). Fine networks of quartz veinlets were observed in some places of the sections studied. Sulfides form disseminated inclusions up to 1 mm in size, as well as veinlets and lenses 0.5–2 cm in length. They are represented by common pyrite and subordinate pyrrhotite, chalcopyrite, arsenopyrite, covellite, and marcasite. Up to 0.1 g/t Au, 0.04 g/t Pt, and 0.01 g/t Pd were previously detected in these rocks by means of semi-quantitative spectral analysis.

3. Analytical methodology

K – Ar dating of biotite was performed through isotopic analysis of argon in a continuous helium flow at the Analytical Center of FEGI FEB RAS, Vladivostok (Table 1). By this method, argon is extracted from a

Table 1
O and H isotopic compositions and K/Ar dating of biotite associated with graphite in the Ruzhino rocks.

Sample	Host rock	δD_{VSMOW}, ‰	$\delta^{18}O_{VSMOW}$, ‰	K, %	Ar_{air}, %	Ar_{rad}., ng/g	Age, Ma
Tg09/2	Granite	−106.7	8.2	6.51	5	177.1 ± 4.5	362 ± 10
Tg09/3	Granite	−82.5	10.1	7.46	2	203.7 ± 6.5	363 ± 13
Tg09/4	Schistose inclusion in granite	−90.1	9.5	6.58	8	144.8 ± 5	298 ± 11

sample by heating with a continuous infrared laser and then separated in a helium flow through a chromatographic capillary column. After that, it is moved via a flow divider into the ion source of a Finnigan MAT-253 mass spectrometer. Measurement of the ^{36}Ar, ^{38}Ar and ^{40}Ar concentrations is performed in the dynamic mode, using an ion detector with three collectors and three electrometric amplifiers (Ignatiev et al., 2009).

Carbon, oxygen and hydrogen isotope measurements were made using a Finnigan MAT-252 mass spectrometer at the Analytical Center of FEGI FEB RAS, Vladivostok. Reproducibility of replicate standards was always better than 0.10‰ for carbon, 0.20‰ for oxygen, and 2‰ for hydrogen (Tables 1 and 2).

Noble-metal concentrations that we focus on are problematic to determine in graphite-bearing rocks. The major difficulty is that graphite, which can capture and hold metals, is chemically inert to almost all chemicals. On the other hand, the concentration values may be significantly lowered by emission of some carbon-metallic complexes that are highly volatile at high temperatures. Because of these characteristics, chemical treatments before inductively-coupled plasma mass spectrometry (ICP-MS) and burning during fire assay routinely used for exploration of the traditional deposits leads to some underestimates of their noble-metal concentrations. Unfortunately, there is no conventional method that can avoid this difficulty and provide an accurate analysis of Au, Ag and PGE in the graphite-bearing rocks. In this situation, we applied miscellaneous analyses to outline the range of noble-metal concentrations in our samples.

The first detections of high Au and Pt contents (Table 3) in the graphite-bearing rocks of Khanka Terrane were obtained using Ion Mass Spectrometry (IMS) at the Institute of Microelectronics and High-Purity Compounds, Russian Academy of Sciences, Chernogolovka (Sikharulidze, 2004). This is a unique analysis allowing a direct high-sensitive detection of elements including noble metals in solid samples. The major advantage of the IMS method is that it does not require a preliminary dissolution of samples in strongly oxidizing reactants. The IMS analysis was conducted using the Element 2 ICP mass spectrometer produced by Thermo Electron Corporation. The spectrometer was equipped with a glow-discharge ion source based on a hollow cathode that was installed instead of the ICP-source sampler (Sikharulidze, 2009). The analysis consisted in the following:

1) A sample was pulverized in a zirconium ball mill into a powder, from which grains less than 100 μm in size were picked up and mixed to homogenize a commonly heterogeneous natural matter;
2) A crater 1.5 mm in diameter and 1 mm in depth, drilled at the end face of a metallic electrode installed in the hollow cathode was filled out under pressure with about 1 mg of the powder required for the analysis.
3) During analysis, the powder was sprayed out and ionized in the glow-discharge plasma. About 100 mass spectrums were obtained for each analysis and then recalculated with the help of software used in the standard ICP procedures to summarize them. Thus, the resulting contents are considered to be mean values calculated based on 100 parallel measurements for each detected element.

Table 2
Carbon isotopic composition in the Ruzhino and Sutyr rocks.

Sample	Material	$\delta^{13}C_{VPDB}$, ‰
Ruzhino		
03–5	Lamprophyre	−8.5
02–1	Graphite disseminated in granite	−8.5
02–4	Granite	−8.7
03–1	Granite	−8.6
03–1a	Graphite veinlet in granite	−8.7
03–3	Schist	−8.6
520	Schist	−10.5
04–22	Shale	−19.9
04–24	Shale	−19.3
04–17	Shale	−25.2
04–34	Shale	−23.7
04–40	Shale	−26.6
Sutyr		
563	Shale	−20.7
561	Shale	−22.7
570	Shale	−21.0
567	Shale	−23.7

Table 3
The IMS analyses (g/t) of the Ruzhino and Sutyr rocks.

Sample	Rock	Ru	Pd	Re	Os	Ir	Pt	Au
Ruzhino								
04–9	Graphite veinlet	n.a.	n.a.	n.a.	n.a.	n.a.	3	2
03–5	Lamprophyre	n.a.	n.a.	n.a.	n.a.	n.a.	52	5
04–7a	Lamprophyre	n.a.	n.a.	n.a.	n.a.	n.a.	20	12
04–29	Lamprophyre	n.a.	n.a.	n.a.	n.a.	n.a.	18	15
03–1a	Granite	n.a.	n.a.	n.a.	n.a.	n.a.	16	5
02–3	Schist	n.a.	n.a.	n.a.	n.a.	n.a.	4	13
03–3	Schist	n.a.	n.a.	n.a.	n.a.	n.a.	7	3
04–7b	Schist	n.a.	n.a.	n.a.	n.a.	n.a.	14	12
04–17	Shale	n.a.	n.a.	n.a.	n.a.	n.a.	5	7
04–40	Shale	n.a.	n.a.	n.a.	n.a.	n.a.	24	17
Sutyr								
562	Shale	14	74	6.0	8.5	7.3	6.1	41
562t	Shale	21	27	9.4	10.2	8.2	9.7	76
564	Shale	25	17	10.4	10.1	7.8	14	72
569	Shale	24	29	7.1	5.2	4.3	12	11
572	Shale	17	41	7.7	8.1	6.4	11	24
574	Shale	22	38	5.2	5.9	3.3	7.8	31
578	Shale	23	80	6.1	12.0	9.2	27	40
593	Shale	6.9	38	3.3	6.4	5.1	3.1	20

n.a. — not analyzed.

The IMS methodology requires improvement such as increasing the rate at which powder is sprayed that controls the analysis sensitivity. This is especially important for graphite, which spraying rate is the slowest among common natural substances. A second impediment that should be overcome is the requirement that samples to be analyzed cannot exceed a minute size. Frequently, geological materials are highly heterogeneous. We have to perform tens of parallel determinations to arrive at representative analytical data. In addition, a set of the IMS standard samples needs to be prepared for exploration.

To confirm the IMS results, representative samples of the graphite-bearing rocks were subjected to the following analyses (Tables 4 and 5):

1. Atomic Absorption Spectrophotometry (AAS) using the Shimadzu AA-6800 and AA-6200 spectrophotometers with electrothermal atomizer at the Analytical Center of the Far East Geological Institute, FEB RAS, Vladivostok, Russia (Table 4). This method sensitivity is 2 ppb for Au, 0.4 ppb for Pd, and 7 ppb for Pt. AAS was applied either directly, through the procedures recommended by the technique producer or after the classical (PbO) fire assay. In addition, this method was used to analyze distribution of Au, Pt and Pd between the easily and sparingly soluble fractions of the Ruzhino graphite-bearing rocks. The relatively soluble fraction was obtained by standard treatment of the samples in $HCl + HNO_3$ (aqua regia) and HF, transferring almost all the silicate components of the rocks into the solution that we analyzed. The graphite-dominated residuals were then subjected to ignition at 600 °C and followed by 30 days-long complete dissolving in the mixture of hydrofluoric, hydrochloric and nitric acids. The resulting carbon-bearing solution was analyzed to determine the extent to which metals are strongly compounded with graphite. All the values obtained were finally recalculated to get total concentrations in a bulk sample.
2. Inductively-Coupled Plasma Mass Spectrometry (ICP-MS) after NiS fire assay and following coprecipitation with Te (Table 5) conducted at the National Geophysical Research Institute, Hyderabad, India,

Table 4
The AAS analyses (g/t) of the Ruzhino rocks.

Sample	Rock	Pd	Pt	Au
04–9[a]	Graphite veinlet	n.a.	0.82	0.14
03–5[a]	Lamprophyre	–	–	1.26
03–5[b]	Lamprophyre	1.24	4.46	1.30
04–6	Lamprophyre	–	0.1	–
04–7a[a]	Lamprophyre	n.a.	1.2	1.0
04–29[a]	Lamprophyre	n.a.	1.3	0.5
02–4[a]	Granite	–	–	0.61
02–4[b]	Granite	1.23	2.39	4.79
04–33	Granite	–	0.1	–
04–88	Granite	0.1	0.1	–
04–18	Skarn	0.1	0.1	0.6
04–77	Skarn	–	0.3	0.1
04–80	Skarn	–	0.2	0.2
04–87	Skarn	–	0.2	0.6
04–107	Skarn	–	0.1	–
04–85	Skarn	0.015	0.055	0.067
04–4[a]	Marble	n.a.	1.29	0.18
02–1[a]	Schist	–	–	0.73
02–1[b]	Schist	5.67	8.68	17.41
02–3[a]	Schist	–	–	0.56
02–3[b]	Schist	0.99	2.15	3.39
03–1a[a]	Schist	–	–	–
03–1a[b]	Schist	3.31	4.14	2.56
03–3[a]	Schist	–	–	0.1
03–3[b]	Schist	7.31	14.15	5.47
04–35	Schist	0.2	–	0.2
04–7b[a]	Schist	n.a.	1.5	0.2
04–13	Schist	0.1	–	–
04–17	Shale	0.04	0.09	0.17
04–17[a]	Shale	n.a.	1.3	0.66
AR–22–4–1[c]	Shale	0.046	0.01	0.42
AR–22–4–2[c]	Shale	0.06	0.01	0.78
AR–34–1[c]	Shale	0.027	0.006	0.48
AR–34–2[c]	Shale	0.016	0.007	0.18
AR–34–3[c]	Shale	0.013	0.005	0.12

Dash — not detected; n.a. — not analyzed.
[a] The Shimadzu AAS-6200 analyses performed after the standard treatment of the samples.
[b] Bulk values resulted from recalculation of the Shimadzu AAS-6200 analyses performed after both standard and additional (ignition at 600 °C and following 30-days long dissolution in HF and $HClO_4$) treatments.
[c] The Shimadzu AAS-6200 analyses performed after the classical (PbO) fire assay. Other data were obtained using Shimadzu AAS-6800 after the standard treatment.

using the ICP-MS ELAN DRC II spectrometer. These analyses represent the most popular method of noble-metal detection in the traditional ores. In addition to the standard treatment, including ignition under 650 °C applied for most samples studied, the ignition was followed by consecutive decomposition in $HCl + HNO_3$, HF, $HClO_4$, and $H_3BO_3HClO_4$ to completely dissolve the residual carbon was used for some samples before ICP MS.

We also studied the rock samples in polished sections, fresh rock chips, and separate grains with the help of the atomic-force microscope Solver P-47 at Institute of Chemistry, FEB RAS, Vladivostok, Russia and scanning electron microscopes EVO-50XVP at Far East Geological Institute, FEB RAS, Vladivostok, Russia and EVO-40XVP at Institute of Tectonics and Geophysics, FEB RAS, Khabarovsk, Russia. Both electron microscopes are equipped with an energy dispersive X-ray spectrometer INCA Energy-350 (SEM EDA analysis, Tables 7–10). The search for and photographing of the noble-metal subjects in polished sections were conducted under the backscattered electron regime, providing an intense glowing of elements with high atomic weights, such as Au and PGE. Some grains of carbon-metallic aggregates were separated from the powdered rock samples after their dissolution in strong acids. The energy dispersive X-ray analysis of microinclusions in both polished sections and separate grains was performed under the secondary electron regime with sensitivity not less than a few wt.% and electron beam diameter of 0.02–0.03 μ. A size of the actually analyzed X-Ray excitation spot is, however, much larger: 2–4 μ in diameter.

In addition, a quantum-chemical modeling of interaction between Au(0), Pt(0), Ag(0) and graphene fragments was undertaken to understand possible forms of noble-metal mineralization in graphite.

Most of the diagrams below were made using the PetroGraph 2beta software (Petrelli et al., 2005).

4. Results

Almost all the rocks are graphitized in both locations studied. Graphite forms disseminated flakes 1–5 mm in size as well as layers, lenses, veins, and veinlets of different thicknesses in crystalline schist, granite, marble, skarn, and lamprophyre in the Ruzhino area. Total carbon content varies from <1% to 36% regardless of the hosted rock type. Schistose graphitic matter with fragments of graphite-bearing rocks frequently mark fractures widely developed in the region. Relationships between graphite and associated minerals are diverse: 1) graphite forms intergrowths with quartz and biotite; 2) graphite veinlets cut biotite aggregates and their clusters; and 3) biotite veinlets cut graphite aggregates and their clusters. These observations suggest that graphite, quartz and biotite form both syn- and post-metamorphic paragenesises. The post-metamorphic origin is more likely for high-grade graphite ores since their occurrences seem to be concentrated around the submeridional fault cutting the regional Pan-African metamorphic zonation. The Late Devonian–Carboniferous K–Ar dates of graphite-associated biotite support this suggestion, although the wide variation of these data indicates a low accuracy of at least one of them (Table 1).

Graphite and associated biotite from the Ruzhino amphibolite-facies rocks is characterized by $\delta^{13}C_{VPDB}$ from −8.5 to −10.5 ‰, δD_{VSMOW} from −82.5 to −106.7 ‰, and $\delta^{18}O_{VSMOW}$ from 8.2 to 10.1 ‰ (Tables 1 and 2), indicating that these rocks have been significantly contributed by a C–O–H mantle-derived fluid (Cartigny et al., 2001; Deloule et al., 1991; Mattey, 1987; Mattey et al., 1994). This suggestion is supported by globular nanostructure of carbon from the highly graphitized granite-gneiss (Fig. 2). In contrast, carbonaceous shales of both Ruzhino and Sutyr areas show $\delta^{13}C_{VPDB}$ from −19.9 to −26.5 ‰

Table 5
The ICP-MS analyses (g/t) of the Ruzhino and Sutyr rocks after different treatments and coprecipitation with Te.

Sample	Rock	Treatment	Ru	Rh	Pd	Os	Ir	Pt	Au
520a	Ruzhino gneiss	NiS fire assay	0.004	0.014	0.043	0.002	0.003	0.12	0.086
521a	Ruzhino gneiss	NiS fire assay	0.008	0.011	0.027	0.002	0.001	0.044	0.066
522b	Ruzhino gneiss	NiS fire assay	0.01	0.007	0.031	–	–	0.06	0.167
552(9)	Sutyr shale	Standard	–	0.0014	0.0316	–	–	0.0005	0.1733
601(7)	Sutyr shale	Standard	0.004	0.0046	0.0111	–	0.0023	0.0054	0.0254
562(3)	Sutyr shale	Standard	–	0.0003	0.107	–	0.001	0.0007	0.033
562(1)	Sutyr shale	$(HCl + HNO_3) + HF + HClO_4 + H_3BO_3$	0.0003	0.0007	0.0153	–	0.0004	0.0271	1.7413
562t(7)	Sutyr shale	Standard	0.0061	0.0066	0.0198	–	0.0061	0.0292	0.2711
562t(2)	Sutyr shale	$(HCl + HNO_3) + HClO_4$	0.0085	0.0133	0.0508	–	0.014	0.1139	2.4983

The Sutyr analyses are averaged (number of analyses shown in the brackets).

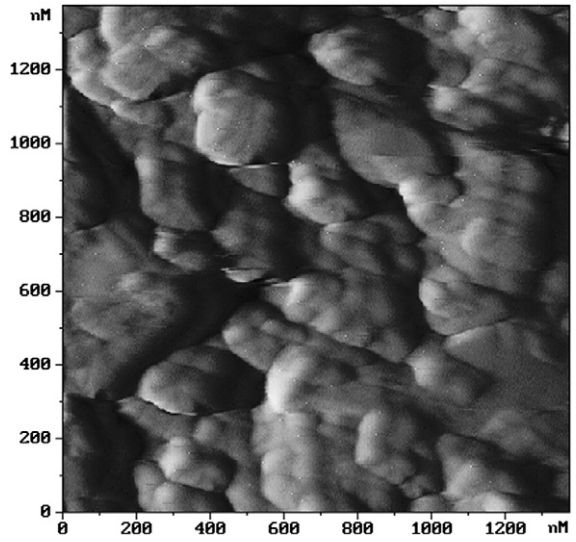

Fig. 2. Globular nanostructure of graphite from the Ruzhino granite–gneiss obtained using the atomic-force microscope Solver P-47 at Institute of Chemistry, FEB RAS, Vladivostok, Russia.

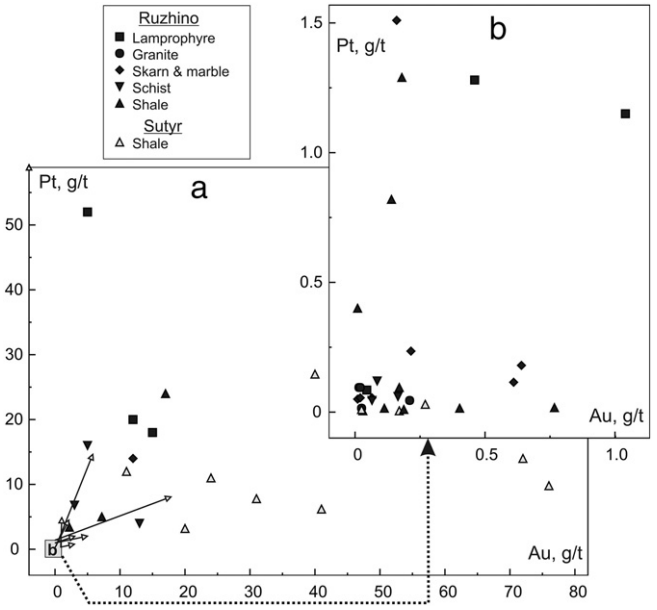

Fig. 3. Au – Pt diagrams of the Ruzhino and Sutyr graphitized rocks: a — the IMS data (Table 3) in comparison with the AAS and ICP-MS data (arrows,Tables 4 and 5) showing a significant increase of the bulk-rock values after the additional chemical treatments of graphite residuals; b — the AAS and ICP-MS data after the standard treatments (Tables 4 and 5).

indicating that their fine dissemination of mostly amorphous carbon is largely of a sedimentary (organic) origin (Schidlowski, 1987).

Noble-metal mineralization like the graphite one was detected in all the rocks studied in the Ruzhino and Sutyr locations. Metal distributions (Tables 3–6, Fig. 3) demonstrate two trends:

1) The IMS analyses that do not require any chemical treatment as well as the AAS and ICP-MS analyses including the severe chemical treatments of the graphite residuals present higher (up to 52 g/t Pt and up to 76 g/t Au) values than the standard AAS and ICP-MS analyses (up to 1.5 g/t Pt and up to 1 g/t Au) especially those made after fire assay (up to 0.12 g/t Pt and up to 0.78 g/t Au);
2) The IMS analyses indicate a higher Pt content in the Ruzhino amphibolite-facies rocks than in the Sutyr carbonaceous shales, while a higher Au content is characteristic of the latter.

Forms of the noble metal-graphite mineralization were thoroughly studied using electron microscopes with energy dispersive X-ray spectrometers. As a result, numerous inclusions were found in graphite and carbonaceous matrix of the Ruzhino rocks, including native metals: gold, copper, zinc, bismuth, nickel, and tungsten; intermetallic compounds: Fe with some Cr admixture, a few kinds of brass (Cu – Zn), bronze (Cu – Sn), and Cu – Sn – Fe; Y – Th – P complexes; Te minerals: $(Sb_{1.7}Bi_{0.3})_2Te_3$, $(Sb_{2.55}As_{0.45})_3Te_3$, and HgTe; Ag minerals: AgI, AgCl, AgBr, Ag(Cl,Br,I), and Hg_3Ag_2; sulfides: Ag_2S, FeS_2, FeAsS, and PbS; oxides: Fe_3O_4, SnO_2, and YPO_4; monazite and other REE. It should be emphasized though that the rocks studied in the Ruzhino location, including those with high contents of C, Au and PGE, are ordinarily sulfide-free. We discovered single accessory microcrystals of pyrite, arsenopyrite, galena and argentite as exotic particles only. This is very unusual, since sulfides are sufficient in most of the known carbon-bearing noble-metal ores.

Among the noble-metal inclusions associated with graphite, gold is found to be the most common. Its grains usually contain different admixtures, including Ag (up to 8 wt.%) and Cu (up to 3 wt.%), but are pure (100% Au) in some spots. Mercurian gold with up to 9 at.% of Hg admixture was also detected in particles up to 1–2 μm in size. In addition, rare complex intermetallic compounds composed of (at.%) 24.5 Au, 10.53 Ag, 58.1 Pd, and 6.87 Sn were found.

The energy dispersive X-ray spectrometry of the largest (1 mm in diameter) spherical gold grain showed significant compositional variations from spot to spot (at.%): 100–79.3 Au, 0–22.02 Ag, 0–2.2 CuO (Fig. 4a). A graphite flake with numerous impurities was detected inside this grain (at. %): 57.92–71.25 C, 0.46–17.4 Au, 28.2–30.3 O, 0.25–2.06 Cl, 0–2.05 K, 0–1.6 Ca, 0–1.7 Si, and 0–1.56 Al. Multicomponent compositions as well as oxygen and chlorine admixtures in the inclusion seem to evidence their co-precipitation from a fluid.

Native gold in skarns differs from that in graphite veinlets and zones of intensive metasomatic graphitization in schists and granite-gneisses by a higher content of silver (up to 10 wt.%) and a larger size of lumpy and spongy grains. One of these grains exposed a carbon nanotube at its surface (Fig. 4b), supporting the suggestion of a simultaneous deposition of gold and carbon from a fluid. It seems to be one of the first records of a carbon nanotube on a natural gold grain. Gold from quartz veins contains W, F and U admixtures.

The Ruzhino lamprophyre dikes of olivine–hypersthene–biotite and garnet–hypersthene–diopside–biotite compositions aroused a special interest because of the anomalously high Pt contents (up to 52 g/t) detected in them by the IMS analysis. No Pt-bearing phase was found though. Meanwhile, lamprophyres are distinguished by significant amounts of accessory zircon, monazite, apatite, orthite,

Table 6
Comparison of Au and Pt contents (g/t) determined by different analyses in the studied graphitized granite–gneiss rocks and carbonaceous shale of the Khanka and Bureya Terranes (based on data from Tables).

Rock	Analysis	No. of samples	Au mean(variation)	Pt mean(variation)
Ruzhino granite–gneiss	FA + ICP-MS	3	0.106(0.066–0.167)	0.075(0.044–0.12)
	AAS	22(17 for Pd)	0.32(0–1.26)	0.34(0–1.5)
	AAS[a]	6	5.82(1.3–17.41)	6.0(2.15–14.15)
	IMS	8	8.38(2–15)	16.75(3–52)
Ruzhino shale	FA + AAS	5	0.4(0.12–0.78)	0.008(0.005–0.01)
	AAS	2(1 for Pd)	0.42(0.17–0.66)	0.7(0.09–1.3)
	IMS	2	12(7–17)	14.5(5–24)
Sutyr shale	ICP-MS	4	0.126(0.033–0.271)	0.009(0.001–0.029)
	ICP-MS[a]	2	2.12(1.741–2.498)	0.07(0.027–0.114)
	IMS	8	39.38(11–76)	11.34(3.1–27)

FA + ICP-MS — NiS fire assay with following ICP-MS; FA + AAS — PbO fire assay with following AAS; n.a. — not analyzed.
[a] Analyses including the additional treatment in strong acids (see Tables 4 and 5 for details); other data present analyses after the standard treatments.

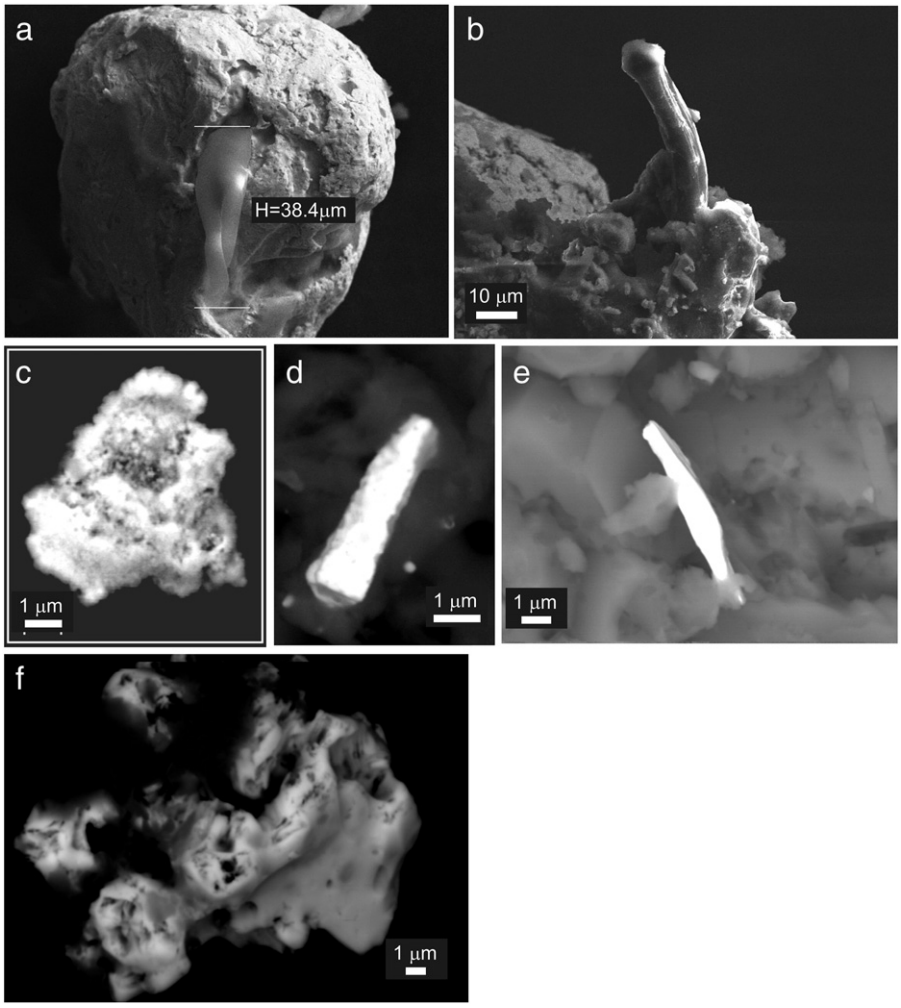

Fig. 4. Microinclusions in the Ruzhino rocks: a — spherical gold grain including a graphite flake; b — carbonaceous nanotube on a gold grain in skarn; c — microaggregate of nanocrystals consisting of Ag compounds with halogens and mercury in the fresh chip of black shale; d — Pt–O–C microinclusion in gneiss (sample 520a); e — the isoferroplatinum wire-shaped particle in black shale (sample 04–17); f — complex Ir-REE aggregate separated after the acidic etching of black shale.

and magnetite. The latter contains 0.08–0.23 wt.% Pt. Zircon is distinguished by high contents of U, Th, and Hf (up to 0.4 at.%). Orthite contains (at.%) 0.8 La, 1.76 Ce, 0.14 Pr, 0.56 Nd, and 0.1 Sm. In addition, this mineral includes phosphorous-bearing uranothorite ($Th_{0.54}U_{0.27}Ca_{0.10}Zr_{0.06}Y_{0.02})_{0.99}Si_{0.9}P_{0.10}$, and REE phosphates (at.%): 15.6 P, 5.55 La, 7.90 Ce, 0.54 Pr, 1.76 Nd, and 0.03 U. These data indicate a possible genetic connection between the revealed noble metal-graphite mineralization and the rare-metal-fluorine ores related to the Paleozoic granites and alkaline rocks located about 50 km to the southwest of the Ruzhino occurrence (Krymsky and Belyatsky, 2001; Sato et al., 2003).

Aggregates of silver compounds with I, Cl, and Hg, having a size of not more than 1–2 μm^2, were found in the Ruzhino black shales. Surveying under magnification of 100,000 times allows a fine heterogeneous structure consisting of different nanoparticles to be recognized in these aggregates (Fig. 4c). Table 7 presents a wide spectrum of compositions detected in different spots of a single silver grain.

Table 7
SEM EDA analyses (wt.%) of Ag compounds with I, Cl, and Hg detected in four spots on a microaggregate from of the Ruzhino black shale.

	1	2	3	4
Ag	49.59	48.22	50.73	53.72
I	50.41	50.37	27.32	46.28
Cl	–	1.41	–	–
Hg	–	–	21.96	–

It was a challenge to find separate grains of platinum-group minerals. We examined numerous polished sections and fresh chips of the Ruzhino rocks, but only two of them showed microinclusions with Pt. Quartz-feldspar gneiss of sample 520a contains a tiny Pt–O–C compound with some Cu and Si admixtures (at.%): 23.17 Pt, 1.87 Cu, 2.08 Si, 31.81 O, and 41.06 C (Fig. 4d). A chip of black-shale (sample 04–17) showed isoferroplatinum (73 at.% Pt, 27 at.% Fe) as a

Table 8
SEM EDA analyses (wt.%) of Ir compounds with C, O, REE, and other elements detected in six spots on a microaggregate from the Ruzhino black shale (Sample 04–17).

	1	2	3	4	5	6
C	68.18	56.21	14.91	40.56	31.60	37.92
O	15.90	22.46	47.43	29.22	29.26	22.70
F	0.59	–	–	–	–	–
Si	0.24	0.29	–	0.32	–	–
Cl	0.16	0.10	–	–	–	–
Co	0.16	–	0.54	0.12	0.64	–
Ni	0.18	–	–	–	–	–
Cu	0.69	0.75	1.17	0.87	1.39	1.18
Br	0.46	–	–	–	–	–
Y	4.75	7.07	12.78	10.85	12.16	13.26
Gd	0.49	0.62	1.04	0.97	1.67	1.20
Dy	0.79	1.11	1.67	1.18	2.85	2.13
Ir	7.41	10.96	20.47	15.67	18.69	21.60
U	–	0.31	–	–	–	–
Yb	–	–	–	–	1.74	–

wire-like inclusion 6 μm in lengh and <1 μm in width (Fig. 4e). In addition, some Ir-REE aggregates of irregular shape (Fig. 4f) were revealed after acidic etching of a fresh chip of black shale. These aggregates consist of fine particles less than 1 μm in size. Table 8 shows their compositions detected in six different microcrystals of a single grain.

The Sutyr carbonaceous shales contain microinclusions of iron, copper, silver, platinum and iridosmium compounds with carbon, oxygen and other elements (Fig. 5).

The iron-predominated inclusions are characterized by admixtures of carbon, oxygen, sulfur, and silicon (wt.%): 56.5–84.3 Fe, 15.7–42.6 C, 5.2–5.3 O, up to 0.3 S, and up to 0.4 Si. The atomic percentage of carbon is 46–73, which is higher than in the natural Fe carbides (25–31 at.%). This along with a heterogeneous character of the grains (Fig. 5a) suggests some additional carbon-dominated mineral phases.

The copper and silver inclusions occur separately and in compounds. The Cu particles are commonly porous, having admixtures of nickel, zinc and carbon (wt.%): 58.5–64.6 Cu, 13.5–14.2 Ni, 17.8–18.0 Zn, and 6.6–10.2 C (Fig. 5b). The silver inclusions are lumpy, containing copper, uranium, zinc, sulfur, silicon, aluminum, oxygen, and carbon (wt.%): 47.8–65.1 Ag, 1.8–20.5 Cu, up to 3.2 U, up to 7.1 Zn, up to 0.5 S, 6.2–3.7 Si, up to 0.8 Al, 5.9–15.1 O, and 7.9–14.6 C (Fig. 5c). The Cu–Ag grains are distinguished by massive structure and plane edges (Fig. 5d). Their cores are occupied by a copper-dominated phase (wt.%): 64.3–64.6 Cu, 14.0–14.1 Ni; 21.3–21.7 Zn. A silver-rich phase

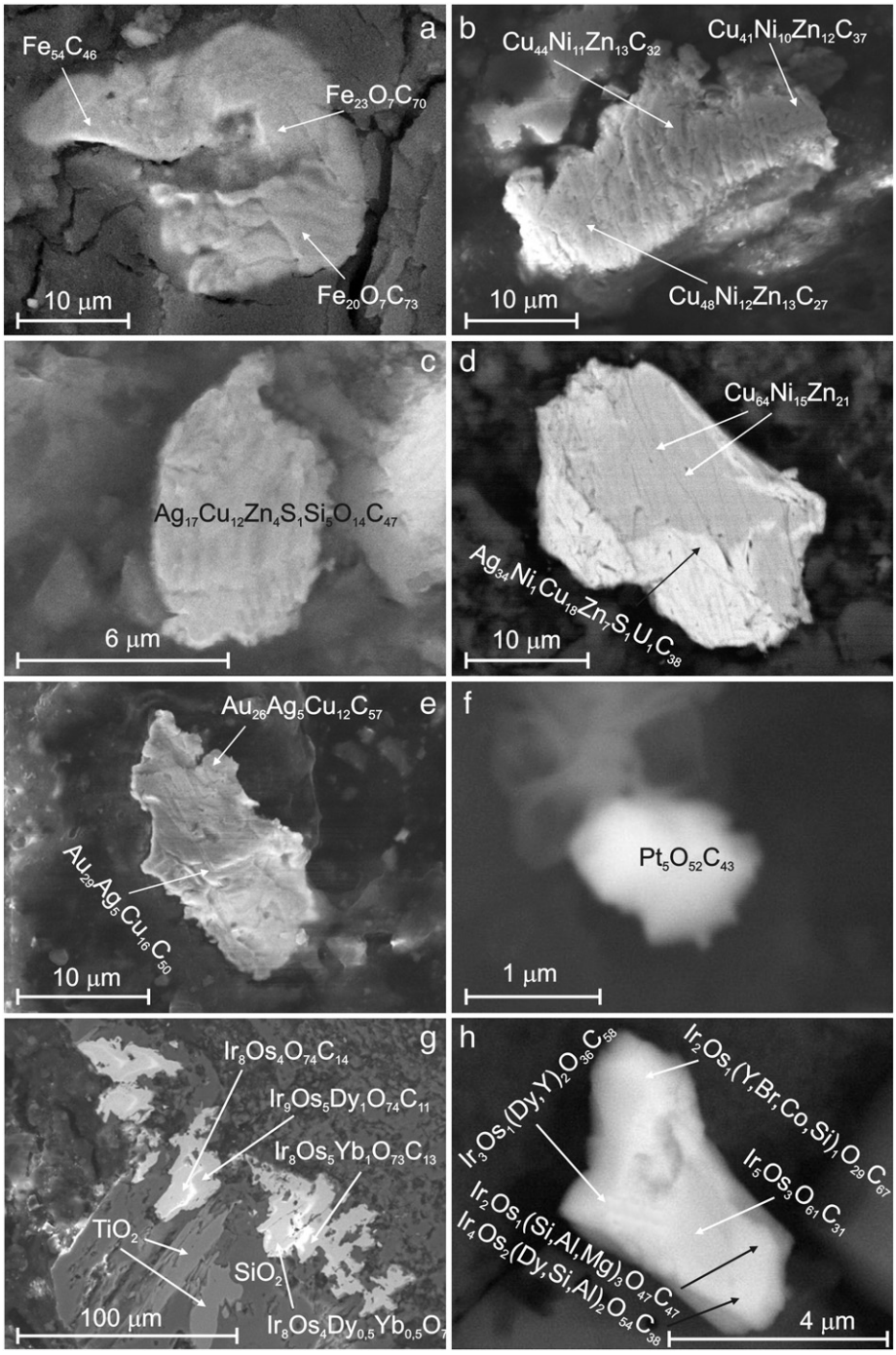

Fig. 5. Microinclusions in the Sutyr carbonaceous shale (sample 552): a–e and g — polished sections, f and h — acidic treatment residuals.

(61.2 Ag, 19.4 Cu, 2.9 U, 0.9 Ni, 7.2 Zn, 0.7 S, and 7.7 C) surrounds the copper-dominated one, evidencing its later origin.

Gold forms flattened grains of irregular shape (Fig. 5e). Its fineness varies between 691 and 724. The admixtures are represented by silver, copper, and carbon (wt.%): 7.3–16.4 Ag, 8.6-12.7 Cu, 3.5-9.6 C.

Platinum-bearing particles were not found in the polished sections, but detected in the carbonaceous residuals formed after a severe acidic treatment of black shales (Fig. 5f). They commonly do not exceed 1–2 μm in size, are lumpy, and have etched shapes. Their compositions are diverse (wt.%): 17–39.1 Pt, 12.3–37.3 O, 23.6–49.6 C, up to 1.6 Fe, up to 1.1 K, up to 0.6 Cl, up to 6.6 Al, up to 0.6 Ti and Mg, and up to 21.7 F (Table 9).

The iridosmium inclusions are intergrown with quartz and rutile and located at the edges of microvoids (Fig. 5g) formed after leaching of sulfides. They have admixtures of dysprosium, ytterbium, oxygen, and carbon (wt.%): 40.2–42.2 Ir, 20.7–23.1 Os, up to 2.9 Dy, up to 2.6 Yb, 26.7–32 O, and 3.1–4.4 C. Many iridosmium grains were extracted from the shales as a result of their acidic treatment. They are much more abundant than gold and platinum. Their composition widely varies between the grains (13 analyses, wt.%): 43.3–11.9 Ir, 20.9–1.8 Os, 50.4–11.2 O, and 63.5–3.6 C; and inside them (Fig. 5h): 33.9–16.4 Ir, 19.2–8.7 Os; 40–24.6 O; 44.4–12 C (Table 10).

The quantum-chemical modeling (Medkov et al., 2010) showed a strong energy of interaction between graphene fragments and clasters of Pt(0), which is 1.5–2.5 times higher than that of Au(0) and Ag(0). In addition, the highest interaction energy was detected for the horizontal platinum clasters laying between the graphite sheets, indicating that they can form so called graphite intercalation compounds (Dunaev et al., 2008). These results theoretically explain why there is no platinum phase visible under electron microscope in the Ruzhino graphitized rocks with high contents of this metal detected by different analyses? The answer is that Pt is almost completely intercalated between the graphite nanosheets. Gold and silver, in contrast, do not have such ability and widely manifest themselves under a microscope. The high energy of Pt – C complexing can also explain a problem with detecting of PGE in graphite-bearing rocks by the ICP MS and AAS analyses using a routine acidic treatment.

5. Discussion

High Au (up to 76 g/t) and PGE (up to 52 g/t Pt, 80 g/t Pd, 25 g/t Ru, 10 g/t Re, 12 g/t Os, and 9 g/t Ir; Table 3) contents detected in the Ruzhino and Sutyr rocks by IMS may be considered as overestimates, since this analytical method is still under development. At the same time, fire assay and standard AAS and ICP MS data indicating less than 1 g/t Au and 1.5 g/t Pt are noticeably underestimated, because the AAS analyses obtained after ignition at 600 °C and severe chemical treatments of graphite residuals show up to 17 g/t Au, 14 g/t Pt, and 7 g/t Pd in the Ruzhino schists (Tables 3 and 6; Fig. 3). These data clearly demonstrate that the Ruzhino amphibolite-facies rocks contain a significant noble-metal resource closely associated with graphite resistant to common chemical treatments. ICP MS after the additional treatments of the Sutyr carbonaceous shales raises Au contents up to 2.5 g/t, while the PGE values increase insignificantly (Tables 5 and 6), indicating that the shales also include a similar hidden resource, the amount of which, however, is considerably lower at least for PGE.

It should be noted that both PbO and NiS fire assays conducted before AAS and ICP MS in some analyses evidently made additional losses of Pt (Tables 4–6). These losses likely resulted from emission of carbon-metallic complexes that become volatile at extremely high temperatures (1000 °C and higher) applied during the fire-assay procedures.

The described microaggregates of Au, Ag, PGE, and other metals with carbon are supposed to be just the visible "tip of an iceberg" with "submerged" mineralization that is much more abundant in the case of Ruzhino. Especially indicative is that we found only a few Pt-bearing microinclusions in the highly graphitized rocks showing high contents of this element. We may deduce from this that a major part of graphite and noble metals form nano and/or molecular complexes, which may not be recognized under the electron microscope. At the same time, the native metals, sulfides and oxides that we can see in both highly graphitized rocks and carbonaceous shales may be

Table 9
SEM EDA analyses (wt.%) of Pt compounds with C, O, and other elements detected in five micrograins from the acidic–treatment residuals of the Sutyr carbonaceous shales (grain 5 is shown in Fig. 10e).

	1	2	3	4	5
C	49.58	35.76	33.64	44.23	23.60
O	25.72	19.35	12.33	14.18	37.28
F	–	21.71	21.12	15.33	–
Mg	–	0.46	0.64	0.33	–
Ti	0.56	–	–	–	–
Al	–	4.05	6.62	3.30	–
Cl	0.56	0.27	–	–	–
K	–	0.67	1.14	0.57	–
Fe	1.31	0.76	1.58	0.92	–
Pt	22.28	16.98	22.93	21.15	39.12

Table 10
SEM EDA analyses (wt.%) of Ir – Os compounds with C, O, and other elements detected eleven times in the same spot of the micrograin separated from the Sutyr carbonaceous shale (Sample 552, Fig. 10h).

	1	2	3	4	5	6	7	8	10	11
C	29.07	63.51	44.40	12.00	30.05	29.94	18.32	6.88	9.10	10.99
O	40.47	16.87	25.06	32.80	24.62	40.03	34.31	11.19	33.21	50.35
Mg	0.74	–	–	–	–	0.53	–	–	–	2.85
Si	1.92	–	0.70	–	–	1.76	1.38	–	–	6.07
K	0.27	–	–	–	–	–	–	–	–	–
F	–	–	–	–	–	–	–	8.10	–	–
Al	–	0.79	–	–	–	1.68	1.13	2.26	–	5.80
Cl	–	0.50	–	–	–	–	–	2.29	–	–
Co	–	–	0.56	–	–	–	–	–	–	–
Br	4.69	–	0.98	–	–	–	–	–	–	–
Y	2.58	4.63	2.33	–	5.77	–	–	–	–	–
Dy	–	–	–	2.11	2.18	–	1.64	6.29	1.52	1.66
Os	6.25	1.81	8.68	19.24	10.27	9.63	15.45	19.69	20.87	8.44
Ir	14.00	11.90	17.30	33.85	27.11	16.42	27.77	43.31	35.30	13.84

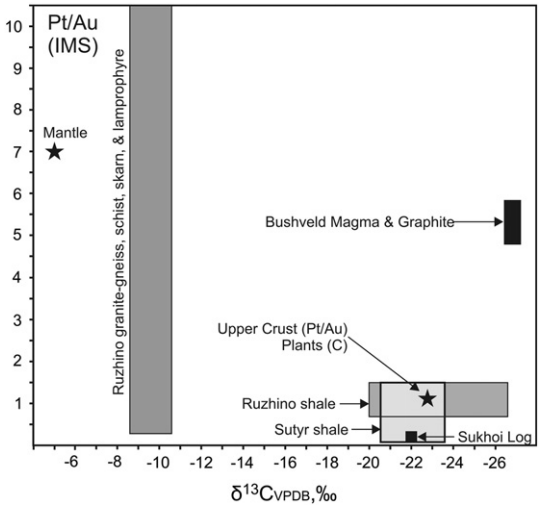

Fig. 6. Pt/Au–$\delta^{13}C$ diagram of the Ruzhino and Sutyr rocks. The reference average compositions are presented for primitive mantle (Barnes and Maier, 1999; Cartigny et al., 2001; Mattey, 1987), upper continental crust (Barnes and Lightfoot, 2005), plants (Schoeninger and DeNiro, 1984), carbonaceous shales of the Sukhoi Log deposit (Distler et al., 2004), Bushveld ore-related magma (Naldrett et al., 2008) and graphite (Harris and Chaumba, 2001).

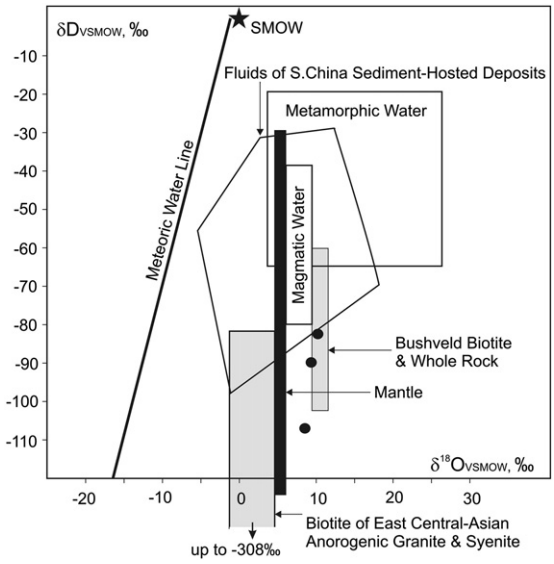

Fig. 7. δD–δ^{18}O diagram of biotite from the Ruzhino granite (black circles) in comparison with biotite and ore-forming fluids of the South China sediment-hosted deposits (Liu et al., 1998; Zhu et al., 1998), East Central-Asian anorogenic granites (Wickham et al., 1996), and Bushveld magmatic complex (Harris and Chaumba, 2001). Fields of magmatic and metamorphic waters were defined by Taylor (1979). The Meteoric Water Line relationship between δD and δ^{18}O is approximately $\delta D = 8 \times \delta^{18}O + 10$ (after Dansgaard, 1964). The mantle field is outlined basing on data from (Deloule et al., 1991; Mattey et al., 1994).

considered as representatives of the traditional sediment-hosted ores. They evidently characterize a minor part of the Ruzhino mineralization, which is detectable by the routine analyses and may be extracted with the help of common ore treatments.

Graphitization of the Ruzhino rocks that was of our special interest can result from either isochemical metamorphism of organic carbon or influx of a carbon-rich fluid. The following data may help to answer, which mechanism was more sufficient.

Fig. 6 shows the Pt/Au via $\delta^{13}C_{VPDB}$ relationship that distinctly distinguishes between mineralizations in carbonaceous shales and the highly graphitized amphibolite-facies rocks. Carbonaceous shales of both locations contain gold associated with organic carbon as a major ore component, like that in the Sukhoi Log deposit (Distler et al., 2004) representing traditional black-shale mineralization in Fig. 6. In contrast, the Ruzhino graphitized rocks are much richer in platinum and associated with mantle-derived carbon.

A sufficient mantle contribution to the mineralization in the Ruzhino amphibolite-facies rocks is confirmed by the isotopic composition of graphite-associated biotite from granite and its schistose xenolith (Fig. 7). δD and δ^{18}O in this mineral markedly differ from those in meteoric and metamorphic waters, as well as fluids of the South China sediment-hosted gold deposits (Liu et al., 1998; Zhu et al., 1998). At the same time, they are close to isotopic compositions of typical magmatic waters and mantle (Deloule et al., 1991; Mattey et al., 1994; Taylor, 1979), as well as magmatic biotites from the Bushveld mafic-ultramafic complex (Harris and Chaumba, 2001) and the East Central Asian anorogenic granite-syenite formations (Wickham et al., 1996). The East Central Asian anorogenic rocks were intruded in the Ordovician–Silurian (~450 Ma), Devonian (~375 Ma), and Permo-Triassic (~280, ~250, and ~220 Ma) times with (Tsygankov et al., 2010) the Devonian and Permian ages corresponding to K–Ar dates of the Ruzhino biotite (Table 1). They are rich in K, like the most graphitized Ruzhino granites and lamprophyres. These data suggest that the Ruzhino noble metal-graphite mineralization is related to the Mid-Paleozoic–Early Mesozoic anorogenic complexes of the Central Asian foldbelt formed under a sufficient mantle influence (Wickham et al., 1996).

Thus, we can distinguish between two processes resulting in the noble-metal mineralizations studied (Table 11). Graphitization with related Pt > Au concentrations of mantle origin are well developed in the Ruzhino amphibolite-facies rocks, while typically crustal hydrothermal alterations and related Au > Pt concentrations are characteristic of the Sutyr carbonaceous shales. These two distinct processes, however, occur close to each other in the Ruzhino area suggesting something common in their origin. The relatively heavy isotopic characteristics ($\delta^{13}C_{VPDB} \sim -10‰$) and high PGE contents (300–1000 g/t Pt) detected in the "insoluble carbonaceous substance" of the Sukhoi Log rocks (Distler et al., 2004; Razvozzhaeva et al., 2008) may be considered as traces of the Ruzhino-type mineralization among the typical sediment-hosted ores.

A significant question is why do the Ruzhino graphite-bearing rocks almost lack sulfides so abundant in many magmatic and sedimentary-hosted ores? We may speculate though that the Ruzhino PGE and some other metals were co-precipitated with carbon, oxygen and halogens from a reduced mantle-derived fluid transporting them in volatile complexes. The deposition occurred in high-temperature conditions, when the fluid was oxidized inside the crustal granite-gneiss complexes. In contrast, the sediment-hosted Au ± PGE ores were originated by an oxidized hydrothermal fluid of heterogenous nature under a reducing influence of the host-rock organic matter. The latter might be a major source of Au as evidenced by numerous studies of the Sukhoi Log and other sediment-hosted deposits (Crespo et al., 2006; Distler et al., 2004; Kao et al., 2001; Kucha, 1981; Varshal et al., 2000 and others).

6. Conclusions

The main question of this research seems to be answered in that we have identified a new type of noble metal-graphite mineralization in the Ruzhino amphibolite-facies rocks. It is characterized by Au and PGE grades as high as those in world-class deposits, but is distinguished from the traditional ores by isotopic compositions of carbon, hydrogen and oxygen, all of which have distinct mantle signatures. Even the Bushveld ores associated with the mantle-derived ultrabasic magmas and related fluids include graphite of organic origin (Harris and Chaumba, 2001; Naldrett et al., 2008). In addition, the Ruzhino rocks are almost free of sulfides, which are characteristic of many sedimentary-hosted and magmatic deposits. The oxides that form some important noble-metal ores are present, but play only a

Table 11
Comparative characteristics of the Ruzhino and Sukhoi-Log (sediment-hosted) mineralizations.

Characteristic	Ruzhino	Sukhoi Log
Host Rocks	Various rocks of the granite–gneiss complexes including anorogenic syenite–granite intrusions	Carbonaceous green–schist rocks forming a metamorphic background of the region
Alteration	Graphite and biotite dissemination and veinlets; skarns	Quartz and sulfide dissemination and veinlets
Isotopic composition of C,O & H	Mantle-derived: $\delta^{13}C_{VPDB}$ from −8 to −11‰; δD_{VSMOW} from −80 to −110‰; $\delta^{18}O_{VSMOW}$ from 8 to 10‰	Crustal: $\delta^{13}C_{VPDB}$ from −20 to −27‰
Pt/Au	>1	<1
Mineral phases	Widely developed "invisible" and chemically resistant nanocompounds between metals and graphite are suggested in addition to some "visible" microinclusions of metals with admixtures of carbon, oxygen, and halogens	The ores are predominated by microinclusions of metals with admixtures of carbon, oxygen, and halogens, among which some residual (?) nanocompounds between metals and graphite occur.

digressive, sidetrack role in the highly graphitized rocks. Other characteristics of the Ruzhino-type mineralization include its association with granite-gneiss complexes and alkaline intrusives in contrast to numerous orogenic gold deposits hosted by greenschist facies rocks and, in some cases, related to crustal granites. However, genetic aspects of this association should be tested by additional geochemical study including appropriate isotopic measurements.

The Ruzhino-type mineralization may be present in the traditional ores, but engaged in the graphite-bound form among the common mineralizations associated with quartz, sulfides and oxides, as reported in the carbonaceous shales studied. Whether it is predominant or concealed by other ores, the Ruzhino-type graphite-based mineralization is extremely resistant. This requires that a special methodology be developed for detection and extraction of the metals. Technologies avoiding a chemical treatment, like Ion Mass Spectrometry, which is under development now, seem to be most appropriate for detection. Meanwhile, a commercial extraction of the metals from such highly resistant substances using severe chemical treatment may invoke additional ecological concerns, while physical procedures like plasma melting may be excessively power-consuming. We will have to develop a new complex processing of the ores, if their resources are proved to be as large as they promise.

Acknowledgements

This study was financially supported by the Russian Foundation for Basic Research (project nos. 11-05-00848a; 11-05-98567) and Presidium of the Far Eastern Branch, Russian Academy of Sciences (Project nos. 09-1-P14-03; 09-2-UO-08-006; 09-1-ON3-03). We thank G.G. Sikharulidze, D.V. Avdeev, Zh.A. Shcheka, V.F. Zanina, S.Yu. Budnitskiy, A.S. Bukatin, S.F. Vasyukevich, and T.A. Ivanova for the geochemical analyses. SEM images and EDA analyses of metals and graphite were made by V.G. Kudryavyi, N.N. Barinov, and P.P. Safonov. We also greatly appreciate the efforts of Hal Strom to improve the language of this paper.

References

Ballhaus, C.G., Stumpfl, E.F., 1985. Occurrence and petrological significance of graphite in the Upper Critical Zone, western Bushveld complex, South Africa. Earth Planet. Sci. Lett. 74, 58–68.

Barnes, S.-J., Lightfoot, P.C., 2005. Formation of magmatic nickel-sulfide ore deposits and processses affecting their copper and platinum-group element contents. In: Hedenquist, J.W., Thompson, J.F.H., Goldfarb, R.J., Richards, J.P. (Eds.), Economic Geology 100th Anniversary Volume, pp. 179–213.

Barnes, S.-J., Maier, W.D., 1999. The fractionation of Ni, Cu, and the noble metals in silicate and sulphide liquids. Geological Association of Canada Short Course Notes, 13, pp. 69–106.

Berdnikov, N., Balaram, V., Cherepanov, A., Avdeev, D., Konovalova, N., Sukharulidze, G., 2010. Some observations on the determination of platinum group elements and gold in black shales. Curr. Sci. 99, 518–521.

Bittencourt, C., Hecq, M., Felten, A., Pireaux, J.J., Ghijsen, J., Felicissimo, M.P., Rudolf, P., Drube, W., Ke, X., Van Tendeloo, G., 2008. Platinum–carbon nanotube interaction. Chem. Phys. Lett. 462, 260–264.

Boudreau, A.E., McCallum, I.S., 1992. Concentration of platinum-group elements by magmatic fluids in layered intrusions. Econ. Geol. 87, 1830–1848.

Cartigny, P., Jendrzejewski, N., Pineau, F., Petit, E., Javoy, M., 2001. Volatile (C, N, Ar) variability in MORB and the respective roles of mantle source heterogeneity and degassing: The case of the southwest Indian. Earth Planet. Sci. Lett. 194, 241–257.

Craw, D., 2002. Geochemistry of late metamorphic hydrothermal alteration and graphitisation of host rock, Macraes gold mine, Otago Schist, New Zealand. Chem. Geol. 191, 257–275.

Crespo, E., Luque, F.J., Rodas, M., Wada, H., Gervilla, F., 2006. Graphite–sulfide deposits in Ronda and Beni Bousera peridotites (Spain and Morocco) and the origin of carbon in mantle-derived rocks. Gondwana Res. 9, 279–290.

Dacheng, J., Ruizhong, H., Yan, L., Xuelin, Q., 2004. Collision belt between the Khanka block and the North China block in the Yanbian Region, Northeast China. J. Asian Earth Sci. 23, 211–219.

Daltry, V.D.C., Wilson, A.H., 1997. Review of platinum-group mineralogy: Compositions and elemental associations of the PG-minerals and unidentified PGE-phases. Mineral. Petrol. 60, 185–229.

Dansgaard, W., 1964. Stable isotopes in precipitation. Tellus 16, 436–463.

Deloule, E., Albarede, F., Sheppard, S.M.F., 1991. Hydrogen isotope heterogeneity in the mantle from ion probe analysis of amphiboles from ultramafic rocks. Earth Planet. Sci. Lett. 105, 543–553.

Distler, V.V., Yudovskaya, M.A., Mitrofanov, G.L., Prokof'ev, V.Y., Lishnevskiy, E.N., 2004. Geology, composition and genesis of the Sukhoi Log noble metals deposit, Russia. Ore Geol. Rev. 24, 7–44.

Dunaev, A.V., Arkhangelsky, I.V., Zubavichus, Ya, Avdeev, V.V., 2008. Preparation, structure and reduction of graphite intercalation compounds with hexachloroplatinic acid. Carbon 46, 788–795.

Harris, C., Chaumba, J.B., 2001. Crustal contamination and fluid–rock interaction during the formation of the Platreef, northern limb of the Bushveld Complex, South Africa. J. Petrol. 42, 1321–1347.

Hulen, J.B., Collister, J.W., 1999. The oil-bearing, Carlin-type gold deposits of Yankee Basin, Alligator Ridge District, Nevada. Econ. Geol. 94, 1029–1050.

Ignatiev, A.V., Velivetskaya, T.A., Budnitskiy, S.Yu., 2009. A method for the determination of argon isotopes in constant helium flow for K/Ar geochronology. Mass Spectrom. 6, 205–213 (in Russian).

Kao, L.S., Peacor, D.R., Coveney Jr., R.M., Zhao, G., Dungey, K.E., Curtis, M.D., Penner-Hahn, J.E., 2001. A C/MoS2 mixed-layer phase (MoSC) occurring in metalliferous black shales from southern China, and new data on jordisite. Am. Mineral. 86, 852–861.

Kaukonen, R., 2008. Sulfide-poor platinum-group element deposits. A mineralogical approach with case studies and examples from the literature: Acta Universitatis Ouluensis A, 516 (134 pp.).

Khanchuk, A.I., 2001. Pre-Neogene tectonics of the Sea-of-Japan region: a view from the Russian side. Earth Sci. 55, 275–291.

Khanchuk, A.I., Plyusnina, L.P., Molchanov, V.P., 2004. The first data on gold-platinoid mineralization in carbonaceous rocks of the Khanka Massif and prediction of a large noble metal deposit in Primorye. Dokl. Earth Sci. 397, 820–824.

Khanchuk, A.I., Plyusnina, L.P., Molchanov, V.P., Medvedev, E.I., 2007. Noble metals in carbon-rich metamorphic rocks of the Khanka terrane, Primorie. Russ. J. Pacif. Geol. 1, 61–70.

Khanchuk, A.I., Berdnikov, N.V., Cherepanov, A.A., Konovalova, N.S., Avdeev, D.V., 2009. First finds of platinoids in black-shale sequences of the Bureya Massif (Khabarovsk Region and Jewish Autonomous Okrug). Dokl. Earth Sci. 425, 213–215.

Khanchuk, A.I., Plyusnina, L.P., Molchanov, V.P., Medvedev, E.I., 2010a. Carbonization and geochemical characteristics of graphite-bearing rocks in the northern Khanka terrane, Primorye, Russian Far East. Geochem. Int. 48, 107–117.

Khanchuk, A.I., Vovna, G.M., Kiselev, V.I., Mishkin, M.A., Lavrik, S.N., 2010b. First results of zircon LA-ICP-MS U-Pb dating of the rocks from the granulite complex of Khanka massif in the Primorye region. Dokl. Earth Sci. 434, 1164–1167.

Krymsky, R.S., Belyatsky, B.V., 2001. The genesis of rare-metal-fluorite mineralization (Voznesenka ore field, Far East, Russia): Nd-Sr isotope constraints. Eleventh Annual V. M. Goldschmidt Conference, Hot Springs, Virginia, Abstract no. 3546.

Kubrakova, I.V., Koshcheeva, I.Ya., Tyutyunnik, O.A., Asavin, A.M., 2010. Role of Organic Matter in the Accumulation of Platinum in Oceanic Ferromanganese Deposits. Geochem. Int. 48, 655–663.

Kucha, H., 1981. Precious metal alloys and organic matter in the Zechstein copper deposits, Poland. Mineral. Petrol. 28, 1–16.

Kucha, H., Plimer, I.R., 1999. Gold in organic matter, Maldon, Victoria, Australia. Econ. Geol. 94, 1173–1179.

Kucha, H., Przybylowicz, W., 1999. Noble Metals in Organic Matter and Clay-Organic Matrices, Kupferschiefer, Poland. Econ. Geol. 94, 1137–1162.

Li, Z., Peters, S.G., 1998. Comparative Geology and Geochemistry of Sedimentary-Rock-Hosted (Carlin-Type) Gold Deposits in the People's Republic of China and in Nevada, USA. USGS Open-File Report, pp. 98–466 (157 pp.).

Liu, J.-M., Liu, J.-J., Zheng, M.-H., Gu, X.-X., 1998. Stable isotope compositions of microdisseminated gold and genetic discussion. Geochimica 27, 585–591 (In Chinese).

Mattey, D.P., 1987. Carbon isotopes in the mantle. Terra Cognita 7, 31–38.

Mattey, D., Lowry, D., Macpherson, C., 1994. Oxygen isotope composition of mantle peridotite. Earth Planet. Sci. Lett. 128, 231–241.

Medkov, M.A., Khanchuk, A.I., Voit, A.V., Plyusnina, L.P., Molchanov, V.P., Medvedev, E.I., 2010. Quantum-chemical study of the interaction between Au(0), Pt(0), Ag(0) and fragments of graphenes modeling graphite structure. Dokl. Earth Sci. 434, 1321–1324.

Melcher, F., Grum, W., Simon, G., Thalhammer, T.V., Stumpfl, E., 1997. Petrogenesis of the ophiolitic giant chromite deposits of Kempirsai, Kazakhstan: a study of solid and fluid inclusions in chromite. J. Petrol. 38, 1419–1458.

Mernagh, T.P., Heinrich, C.A., Leckie, J.F., Carville, D.P., Gilbert, D.J., Valenta, R.K., Wyborn, L.A.I., 1994. Chemistry of low-temperature hydrothermal gold, platinum, and palladium (±uranium) mineralization at Coronation Hill, Northern Territory, Australia. Econ. Geol. 89, 1053–1073.

Mishkin, M.A., Khanchuk, A.I., Zhuravlev, D.Z., Lavrik, S.N., 2000. First data on the Sm–Nd systematics of metamorphic rocks in the Khankai Massif, Primor'e region. Dokl. Earth Sci. 375, 1283–1285.

Mogessie, A., Stumpfl, E.F., Weiblen, P.W., 1991. The role of fluids in the formation of platinum-group minerals, Duluth Complex, Minnesota; mineralogic, textural, and chemical evidence. Econ. Geol. 86, 1506–1518.

Naldrett, T., Kinnaird, J., Wilson, A., Chunnett, G., 2008. Concentration of PGE in the Earth's Crust with Special Reference to the Bushveld Complex. Earth Sci. Front. 15, 264–297.

Pasava, J., 1993. Anoxic sediments—an important environment for PGE; an overview. Ore Geol. Rev. 8, 425–445.

Petrelli, M., Poli, G., Perugini, D., Peccerillo, A., 2005. Petrograph: a new software to visualize, model, and present geochemical data in igneous petrology. Geochem. Geophys. Geosyst. 6, Q07011 (15 pp).

Plyusnina, L.P., Kuz'mina, T.V., Likhoidov, G.G., Narnov, G.A., 2000. Experimental modeling of platinum sorption on organic matter. Appl. Geochem. 15, 777–784.
Plyusnina, L.P., Kuz'mina, T.V., Avchenko, O.V., 2004. Modeling of gold sorption on carbonaceous matter at 20–500°C and 1 kbar. Geochem. Int. 42, 755–763.
Plyusnina, L.P., Kuz'mina, T.V., Safronov, P.P., 2009. Bitumen-graphite transformation (data of experimental modeling). Dokl. Earth Sci. 425, 307–310.
Razvozzhaeva, E.A., Nemerova, V.K., Spiridonova, A.M., Prokopchuk, S.I., 2008. Carbonaceous substance of the Sukhoi Log gold deposit (East Siberia). Russ. Geol. Geophys. 49, 371–377.
Sato, K., Suzuki, K., Nedachi, M., Terashima, S., Ryazantseva, M.D., Vrublevsky, A.A., Khanchuk, A.I., 2003. Fluorite deposits at Voznesenka in the Khanka Massif, Russia: geology and age of mineralization. Resour. Geol. 53, 193–211.
Schidlowski, M., 1987. Application of stable isotopes to early biochemical evolution on Earth. Annu. Rev. Earth Planet. Sci. 15, 47–72.
Schoeninger, M.J., DeNiro, M.J., 1984. Nitrogen and carbon isotopic composition of bone collagen from marine and terrestrial animals. Geochim. Cosmochim. Acta 48, 625–639.
Sener, A.K., Grainger, C.J., Groves, D.I., 2002. Epigenetic gold–platinum-group element deposits: examples from Brazil and Australia. Appl. Earth Sci. 111, B65–B73(9).
Sikharulidze, G.G., 2004. Ionic source with a hollow cathode for element analysis of solids. Mass-Spektrometriya 1, 21–30 (in Russian).
Sikharulidze, G.G., 2009. Modernization of the Element 2 mass spectrometer. Instrum. Exp. Tech. 52, 242–244.
Solonenko, V.P., 1951. Geology of graphite deposits in the East Siberia and Far East. Izdatel'stvo Geologicheskoy Literatury, Moscow (382 pp. (in Russian)).
Taylor Jr., H.P., 1979. Oxygen and hydrogen isotope relationships in hydrothermal mineral deposits, In: Barnes, H.L. (Ed.), Geochemistry of Hydrothermal Ore Deposits, 2nd ed. John Wiley and Sons, New York, pp. 236–277.
Tressaud, A., Hagenmuller, P., 2001. Graphite intercalation compounds of platinum–metal and gold fluorides. J. Fluor. Chem. 111, 221–225.
Tsygankov, A.A., Litvinovsky, B.A., Jahn, B.M., Reichow, M.K., Liu, D.Y., Larionov, A.N., Presnyakov, S.L., Lepekhina, Ye.N., Sergeev, S.A., 2010. Sequence of magmatic events in the Late Paleozoic of Transbaikalia, Russia (U–Pb isotope data). Russ. Geol. Geophys. 51, 972–994.
Varshal, G.M., Velyukhanova, T.K., Chkhetiya, D.N., Kholin, Yu.V., Shumskaya, T.V., Tyutyunnik, O.A., Koshcheeva, I.Ya., Korochantsev, A.V., 2000. Sorption on humic acids as a basis for the mechanism of primary accumulation of gold and platinum group elements in black shales. Lithol. Miner. Resour. 35, 538–545.
Volborth, A., Housley, R.M., 1984. A preliminary description of complex graphite, sulphide, arsenide, and platinum group element mineralization in a pegmatoid pyroxenite of the Stillwater complex, Montana, U.S.A. Mineral. Petrol. 33, 213–230.
Wickham, S.M., Albertz, A.D., Zanvilevich, A.N., Litvinovsky, B.A., Bindeman, I.N., Schauble, A., 1996. A stable isotope study of anorogenic magmatism in East Central Asia. J. Petrol. 37, 1063–1095.
Wilde, S., Wu, F., 2003. The Siberian-North China collision: new geochronological evidence from the Jiamusi and Khanka Massifs. Precambrian Res. 122, 311–327.
Wright, A.J., Parnell, J., Ames, D.E., 2010. Carbon spherules in Ni–Cu–PGE sulphide deposits in the Sudbury impact structure, Canada. Precambrian Res. 177, 23–38.
Wu, F.Y., Yang, J.H., Lo, C.H., Wilde, S.A., Sun, D.Y., Jahn, B.M., 2007. The Heilongjiang Group: a Jurassic accretionary complex in the Jiamusi Massif at the western Pacific margin of northeastern China. Island Arc 16, 156–172.
Zhou, J.B., Wilde, S.A., Zhao, G.C., Zhang, X.Z., Wang, H., Zeng, W.S., 2010. Was the easternmost segment of the Central Asian Orogenic Belt derived from Gondwana or Siberia: an intriguing dilemma? J. Geodyn. 50, 300–317.
Zhu, L.M., Liu, X.F., Jin, J.F., He, M.Y., 1998. The study of the time-space distribution and source of ore-forming fluid for the fine-disseminated gold deposits in the Yunnan–Guizhou–Gangxi area. Sci. Geol. Sin. 33, 463–473 (in Chinese).